

Phase and reflectivity behavior near the excitation of surface plasmon polaritons in Kretschmann-ATR systems with metamaterials

M.A. Zeller, M. Cuevas^a, and R.A. Depine

Grupo de Electromagnetismo Aplicado, Instituto de Física de Buenos Aires, Facultad de Ciencias Exactas y Naturales, Universidad de Buenos Aires and Consejo Nacional de Investigaciones Científicas y Técnicas (CONICET), Ciudad Universitaria, Pabellón I, C1428EHA, Buenos Aires, Argentina

Received 23 August 2011 / Received in final form 2 November 2011

Published online 25 January 2012 – © EDP Sciences, Società Italiana di Fisica, Springer-Verlag 2012

Abstract. In this work we study the optical response of Kretschmann-ATR structures with metamaterials near conditions of resonant coupling between the incident wave and a surface plasmon polariton. In contrast with previous research available in the literature, particular attention is paid to the behavior of the phase of the reflected fields. Besides, the results are discussed in the frame of a phenomenological model based on the properties of the complex poles and zeroes of the reflection coefficient.

1 Introduction

Surface plasmon polaritons (SPPs) are electromagnetic surface waves [1,2]. The necessary condition for their existence on a flat surface between homogeneous media is that the media on both sides of the surface should have a constitutive parameter (electric permittivity or magnetic permeability) with opposite signs. The localization provided by SPPs is very attractive for many applications such as data storage, microscopy, light generation or biophotonics [3]. The most studied case in the literature [1,2,4,5] is that of metal-vacuum interfaces, where opposite signs occur because of the negative electric permittivity of the metal. Comparatively much less attention has been paid to the case of SPPs on metamaterial-vacuum interfaces, where the metamaterial [6,7] can provide negative values to the electric permittivity or magnetic permeability, despite the fact that SPPs on metamaterial surfaces may have very different characteristics [8] from those of SPPs on metallic surfaces. The most significant differences are manifested in the polarization and the direction of energy propagation. Whereas flat metallic surfaces can only support p polarized SPPs, flat metamaterial surfaces can support both p and s polarized SPPs, depending on the values taken by the constitutive parameters at the operating frequency. Analogously, in the metal case the direction of energy propagation is always parallel to the direction of wave propagation, while in the metamaterial case the direction of energy propagation can be either parallel or antiparallel to the direction of wave propagation [9].

Since the spatial periodicity associated with SPPs is less than the spatial periodicity which could be induced

by an incident photon on the surface, SPPs cannot be resonantly excited by plane waves. This difficulty can be overcome by using phase-coupling techniques which give the photon the additional momentum increase needed to achieve SPP excitation. One of the most popular coupling techniques is based on the use of attenuated total reflection (ATR). This technique requires the introduction of a second surface, usually the base of an isosceles prism [10,11], as shown in Figure 1 for the Kretschmann configuration. A SPP can be excited along the interface 2-3 when the incident radiation reaches the base of the prism (interface 1-2) with an angle θ greater than the critical angle of total reflection. In this situation, the evanescent field can resonantly couple with the SPPs of the interface 2-3 and the excitation is manifested as a pronounced minimum in the curves of reflectivity vs angle of incidence.

It is clear that SPPs involved in ATR experiments are not strictly the same as those obtained for the case of a single flat surface. For this reason, the correct interpretation of ATR experiments requires to consider *three* media instead of two. As in any resonant problem, the study of SPPs in ATR structures can be approached in two different but complementary ways: (i) by studying the non-trivial solutions to the boundary value problem in the absence of external sources (homogeneous problem, or mode approach) or (ii) by studying the electromagnetic response of the ATR structure when excited by an external source (direct problem, or reflectivity approach). The first approach has already been considered in reference [12], where we presented a detailed study of the kinematic and dynamic characteristics of SPPs in Kretschmann-ATR systems with a metamaterial medium. The interested reader can also find in that work [12] a review of the last findings

^a e-mail: cuevas@df.uba.ar

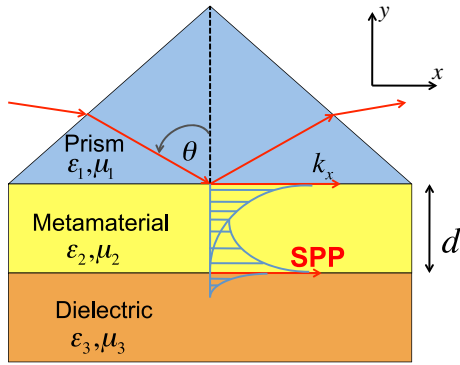


Fig. 1. (Color online) Configuration.

related to SPPs in ATR systems with metamaterials. The purpose of this paper is threefold: (a) to address the second approach; (b) to exhibit the complex optical response of the ATR structure and (c) to highlight similarities and differences between the results obtained with the mode and the reflectivity approaches. Unlike similar studies by other authors [13–18], focusing exclusively on the study of the reflectivity curves, in the present work we correlate the behavior of the reflectivity with the phase behavior of the reflected field. We believe that the inclusion of the phase is attractive because it is an easily accessible magnitude, both experimentally and theoretically. Moreover, the phase can provide additional information not provided by the reflectivity, as has been shown for other resonant phenomena analogous to those considered here [19–21]. Another novel aspect of this work is the presentation of a phenomenological model. Unlike the rigorous electromagnetic model, which is hardly able to provide a priori information, we show that the phenomenological model can accurately exhibit the main characteristics of the electromagnetic response of ATR structures with metamaterials in a very simple manner. This phenomenological model – a generalization to metamaterials of the model used in the metal case to study resonant processes in grating couplers [22] and ATR structures [20] – is based on the knowledge of two complex parameters characteristic of the structure and independent of the incident angle: the zeroes and poles of the reflection coefficient. These two parameters can be obtained by fitting experimental curves of reflectivity and phase vs angle of incidence, as showed in the analogous case of diffraction gratings formed by metamaterials [21]. Alternatively, both parameters can be obtained numerically, an approach that requires the analytic continuation to the complex plane of the electromagnetic formalism used to find the response curves. Taking advantage of the facts that (i) the details of the analytical continuation and (ii) the numerical method to calculate the propagation constant of the SPPs, have been previously developed in [12], this is the approach we used in this work.

The plan of this paper is as follows. In Section 2 we give the rigorous expressions used to calculate the complex amplitude of the reflected fields in the Kretschmann-ATR configuration, we present the phenomenological model and

we show how to use the curves of phase vs. angle of incidence to obtain additional information – not provided by the reflectivity curves – about the existence of critical thicknesses for which the incident wave is totally absorbed by the structure ATR via the resonant excitation of SPPs. Since we have chosen to perform our study by fixing the frequency of the incident wave while varying other parameters such as the angle of incidence and the thickness of the metamaterial, dispersion is irrelevant here. In Section 3 we investigate the influence of the SPP-photon coupling in the response (reflectivity and phase) of the ATR structure for the same regimes considered in [12] for the study of the homogeneous problem. In addition, we calculate numerically the parameters of the phenomenological model and we show that the model reproduces in a very satisfactory manner the behavior predicted by the rigorous electromagnetic formalism. Finally in Section 4 we summarize and discuss the results obtained.

2 Theory

Figure 1 shows the Kretschmann-ATR structure. It is illuminated by a linearly polarized monochromatic plane wave incident from medium 1 (the prism) with an angle θ greater than the critical angle of total reflection. Medium 2 is a metamaterial with negative values of electric permittivity ε_2 and magnetic permeability μ_2 in contact with two non-magnetic dielectric materials ($\mu_1 = \mu_3 = 1$) with real and positive electric permittivities (ε_1 and ε_3). The system of coordinates is chosen so that the x axis coincides with the propagation direction of the SPP and the y axis is perpendicular to the interfaces. For p -polarization the magnetic field vector of the incident wave is parallel to the z axis while for s -polarization the electric field vector of the incident wave is parallel to the z axis. We assume a harmonic time dependence of the fields in the form $e^{-i\omega t}$, with ω the angular frequency of the monochromatic plane wave, t the time and $i = \sqrt{-1}$. Under these hypotheses, the complex amplitude r_1 of the fields reflected in medium 1 can be obtained by following steps formally similar to those already presented to calculate the magnitude denoted by the same name in the homogeneous problem [12], replacing the homogeneous system (Eq. (2) in [12]) with an inhomogeneous system which takes into account the presence of the incident wave. After solving the new system

$$r_1 = \frac{r_{12} + r_{23} e^{2i\beta_2 d}}{1 + r_{12} r_{23} e^{2i\beta_2 d}}, \quad (1)$$

where $r_{ij} = \frac{Z_i - Z_j}{Z_i + Z_j}$, $i, j = 1, 2, 3$, is the reflection coefficient corresponding to a single surface between media i and j , d is the thickness of the metamaterial, $\beta_j^2 = (\frac{\omega}{c})^2 \varepsilon_j \mu_j - \alpha^2$, $Z_j = \beta_j / \sigma_j$ and $\sigma_j = \varepsilon_j$ for p -polarization or $\sigma_j = \mu_j$ for s -polarization. We believe that at this point it is relevant to note that certain magnitudes involved in this work and in [12] have very different physical interpretations, although we are using identical notation to exploit the

formal similarity. For example, the complex amplitude r_1 in the problem of modes represents the amplitude of an evanescent wave in the y direction, while here it represents the amplitude of the reflected wave, i.e., a propagating wave in the y direction. Similarly, in the problem of modes α is a complex magnitude that represents the propagation constant of an SPP and its value is obtained by requiring the denominator in equation (1) to be zero, whereas in the problem schematized in Figure 1, α takes a real value imposed by the incident wave

$$\alpha = \frac{\omega}{c} \sqrt{\varepsilon_1 \mu_1} \sin \theta, \quad (2)$$

where c is the speed of light in vacuum. The necessary condition to obtain a coupling between the incident wave and the SPP propagating along the surface 2–3 with complex propagation constant α_{23} is

$$\frac{\omega}{c} \sqrt{\varepsilon_1 \mu_1} \sin \theta = \text{Re } \alpha_{23}. \quad (3)$$

When this condition holds, we expect an energy transfer from the incident wave to the SPP and therefore a decrease in the reflectivity of the system. We also expect this reflectivity decrease to be more or less pronounced, depending on the thickness d of the metamaterial. We see that it is not easy to predict the details of the expected behavior from the reflectivity of the system $|r_1|^2$ given by equation (1). For this reason it is convenient to resort to a phenomenological model originally used to describe the SPP resonant response in metallic gratings [19,22] and extended to ATR metal devices [20] and to metamaterial gratings [21]. According to this model, the complex amplitude of the reflected wave in medium 1 has the following expression

$$r_1(z, d/\lambda) = \zeta(z, d/\lambda) \frac{z - z_0(d/\lambda)}{z - z_p(d/\lambda)}, \quad (4)$$

where z is the analytic continuation of $\sin \theta$ to the complex plane, z_0 and z_p denote respectively the complex zero and pole of r_1 and $\zeta(z, d/\lambda)$ is a complex regular function near z_0 and z_p that does not change remarkably near z_p . With the choice of the complex variable $z = \sin \theta$, and as seen in [12], the value z that makes the denominator in equation (1) zero (i.e. the pole $z = z_p$) is the ratio between the dimensionless propagation constant $\kappa(d/\lambda) = c \alpha(d/\lambda)/\omega$ and the index of refraction of the medium 1,

$$z_p(d/\lambda) = \kappa(d/\lambda)/\sqrt{\varepsilon_1 \mu_1}. \quad (5)$$

The complex numbers z_0 and z_p depend on the constitutive parameters and on the thickness d and must be calculated numerically as the zeroes of the numerator and denominator of equation (1) respectively. As the value of d is changed, the positions of the zero and the pole determine two trajectories in the complex plane. For physical reasons, the pole trajectory cannot cross the real axis. If it did, infinite reflectance would result for some real angle of incidence. The trajectory of the zero, on the other hand, is not limited and in principle it could cross the real

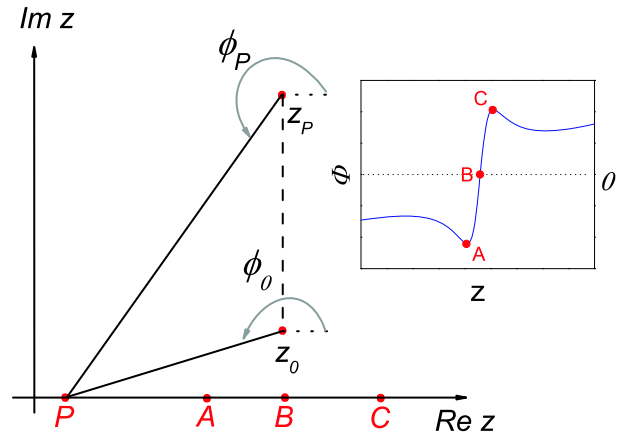


Fig. 2. (Color online) Phase shift ϕ as a function of $z = \sin \theta$ for $\text{Im}(z_0) \text{Im}(z_p) > 0$.

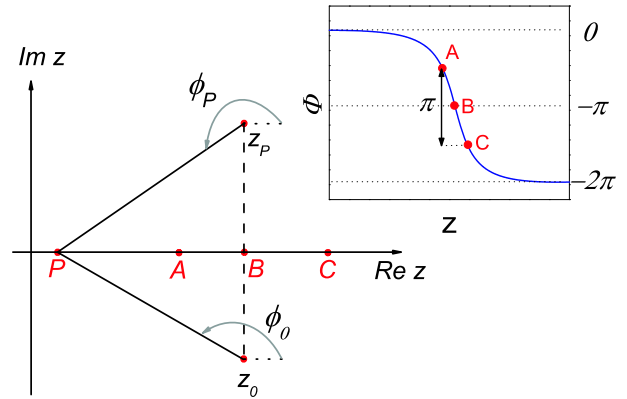


Fig. 3. (Color online) Phase shift ϕ as a function of $z = \sin \theta$ for $\text{Im}(z_0) \text{Im}(z_p) < 0$.

axis for some critical value of d/λ . The existence of this critical value has been experimentally verified in diverse circumstances [20,23–25] and the phenomenon is known in the literature as *total absorption*.

We will see below that the phase of the reflected field plays an important role in the search for a critical value of d/λ for which z_0 is purely real. In the frame of the phenomenological model, and to within an additive constant, the phase of r_1 is given by the following expression

$$\phi(z, d/\lambda) = \arctan \frac{z - z_0}{z - z_p}. \quad (6)$$

Equation (6) shows that $\phi(z, d/\lambda)$ can exhibit very different behaviors as a function of $z = \sin \theta$ (i.e. real z) depending on the location in the complex plane of the imaginary parts of both the zero and the pole. To illustrate these behaviors, in Figures 2 and 3 we show two situations: $\text{Im}(z_0) \text{Im}(z_p) > 0$ (Fig. 2) and $\text{Im}(z_0) \text{Im}(z_p) < 0$ (Fig. 3). For simplicity, and given that in the case of highly symmetrical response curves (as in the metallic case) it has always been observed that $\text{Re } z_0 \approx \text{Re } z_p$, in Figures 2 and 3 we assumed that the zero and the pole have the same real parts. If this condition does not hold for metamaterial structures, the corresponding response

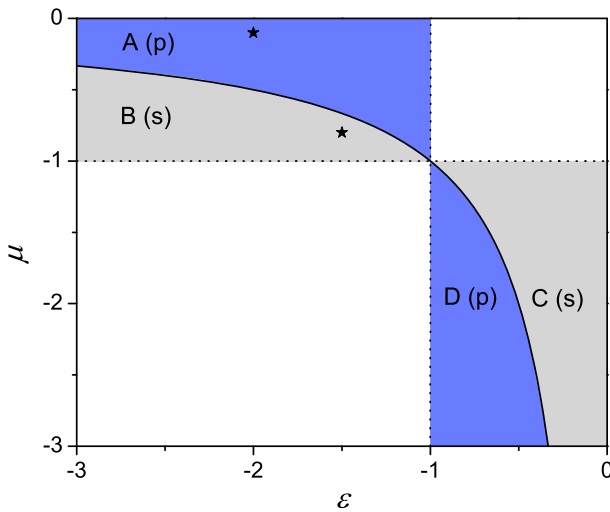


Fig. 4. (Color online) SPPs regimes for a flat interface between a lossless metamaterial with arbitrary values of electric permittivity and magnetic permeability (ε_2, μ_2) and a lossless, conventional material (ε_3, μ_3). The axis are $\varepsilon = \varepsilon_2/\varepsilon_3$ and $\mu = \mu_2/\mu_3$. The values used in the examples are indicated by stars.

curves would display a loss of symmetry without changing, however, the general conclusions of the present discussion. Let us consider a real value of z as indicated by the point P in Figure 2. Taking into account that the phase $\phi(z, d/\lambda)$ given by equation (6) is represented by the difference between angles ϕ_0 and ϕ_p indicated in Figure 2, by moving P along the real axis it is possible to visualize the behavior of $\phi = \phi_0 - \phi_p$ for different angles of incidence. The result is shown in the inset in Figure 2: $\phi \rightarrow 0$ when $|z| \gg \text{Im}(z_p)$, $\phi < 0$ when P is on the left of B , $\phi > 0$ when P is on the right of B and $\phi = 0$ when $P = B$. Note that the phase curve exhibits a minimum for $P = A$ and a maximum for $P = C$. Repeating a similar analysis for the case $\text{Im}(z_0)\text{Im}(z_p) < 0$ (see Fig. 3), we observe that the phase curve is now a monotonically decreasing function of the angle of incidence. Taking into account that the results shown in Figures 2 and 3 indicate that the phase curves as a function of $z = \sin \theta$ have a very different behavior before and after the zero crosses the real axis – i.e., before and after the metamaterial thickness reaches the critical value d/λ for which a total absorption is expected – we conclude that the observation of the phase curves vs θ obtained for different values of d/λ allows us to visualize the position of the zero in the complex plane. We note that this information cannot be extracted from the reflectivity curves only.

3 Results

In this section we analyze the reflectivity and phase curves as functions of the angle of incidence for different values of the geometrical parameters of the ATR system. To correlate these curves with the results obtained in the study of the problem of modes, we have chosen constitutive

parameters with values identical to those used to illustrate the new regimes of SPPs associated with almost transparent metamaterials with negative index of refraction [12]. For the metamaterial medium these values are located in regions A and B of the $\varepsilon - \mu$ diagram shown in Figure 4. The constitutive parameters of medium 1 correspond to a prism ($\varepsilon_1 = 2.25, \mu_1 = 1$) and those of medium 3 to a vacuum ($\varepsilon_3 = 1, \mu_3 = 1$). To complete the analysis we show the parametric trajectories of the zero and the pole in the complex plane, with the dimensionless thickness d/λ as a parameter. For the systematic search of the complex zeros of both the numerator and denominator in equation (1) we have used the efficient numerical formalism already implemented to find those propagation constants of SPPs in ATR systems [12].

3.1 Case 1: p -polarization, forward SPPs

In our first example, the metamaterial constitutive parameters are $\varepsilon_2 = -2 + i 0.001$ and $\mu_2 = -0.1 + i 0.001$, located in region A shown in Figure 4. This region corresponds to p -polarized, forward SPPs. In the limit $d \rightarrow \infty$, the dimensionless propagation constant is $\kappa_\infty = 1.12546 + i 0.00046$. Assuming $\kappa(d/\lambda) \approx \kappa_\infty$, equation (3) predicts a resonant coupling between the SPP and the incident wave at an angle of incidence $\theta \approx 48^\circ$. Figure 5 shows plots of reflectivity $|r_1(\theta)|^2$ and phase $\phi(\theta)$ for different values of the thickness to wavelength ratio d/λ in the range 0.38–0.68. From the reflectivity curves (Fig. 5a) we note that both the angular position of the minimum and the angular width of the resonances depend on d/λ . The increase in the angular position of the minimum when the value of d/λ is varied from 0.38 to 0.68 indicates an increase in the real part of the polariton propagation constant, in total agreement with the results predicted by the homogeneous problem (see Fig. 3a in [12]). In the same way, the decrease in the angular width of the resonances when the value of d/λ is varied in the same interval indicates a decrease in the imaginary part of the polariton propagation constant, a fact which is again in total agreement with the results predicted by the homogeneous problem (see Fig. 3b in [12]). Almost identical reflectivity curves with very pronounced dips (computed minima $\approx 10^{-6}$) can be observed for $d/\lambda = 0.5540$ and $d/\lambda = 0.5545$. Although both reflectivity curves are indistinguishable in the scale of Figure 5a, the phase curves obtained for these thicknesses exhibit very different behaviors. The phase curves for $d/\lambda = 0.5540$ and for $d/\lambda = 0.3800$ are decreasing functions of the angle of incidence, whereas for $d/\lambda = 0.5545$ and for $d/\lambda = 0.6800$ the phase exhibits a minimum and a maximum.

The change of behavior in the phase curves cannot be easily explained by the rigorous theoretical model. However, it can easily be interpreted in the frame of the pole-zero phenomenological model, since, according to the above discussion, this change of behavior would indicate the existence of a critical value of d/λ , between the values 0.5540 and 0.5545, for which the zero of the reflection

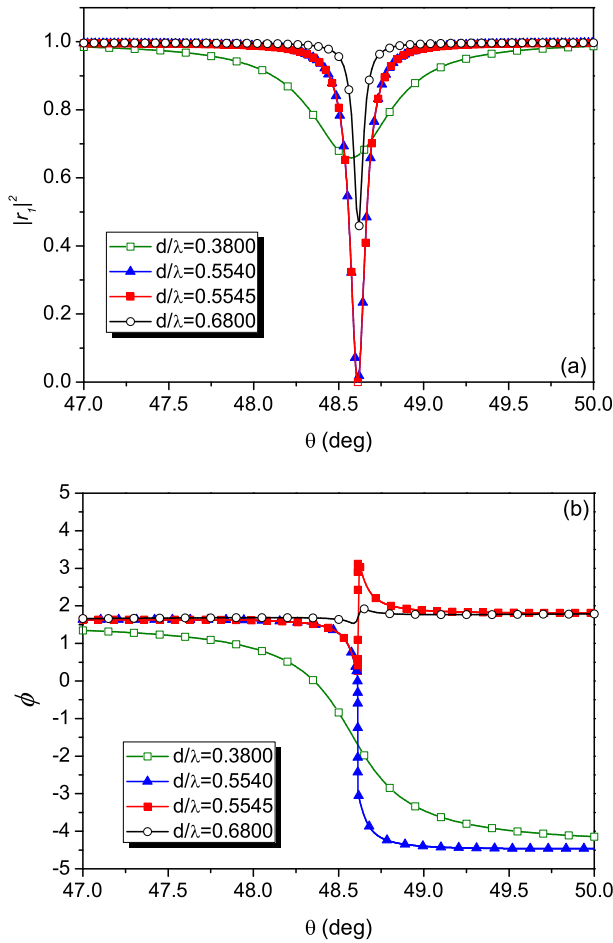


Fig. 5. (Color online) (a) Reflectivity $|r_1(\theta)|^2$ and (b) phase shift $\phi(\theta)$ as functions of the angle of incidence θ and for different values of the thickness to wavelength ratio d/λ . The relative constitutive parameters correspond to regime A.

coefficient crosses the real axis thus allowing a total absorption of the incident energy by the ATR structure. The phase curves shown in Figure 5b for $d/\lambda \leq 0.5540$ are decreasing functions of the angle of incidence, which is in agreement with the behavior predicted by the phenomenological model for $\text{Im}(z_0)\text{Im}(z_p) < 0$ (see Fig. 3) and indicates that in this thickness range $\text{Im}(z_0) < 0$, since a forward SPP should have the imaginary part of its propagation constant, i.e. the imaginary part of the pole, positive [12]. Analogously, we see that the behavior of the phase curves for $d/\lambda \geq 0.5545$ indicates that in this thickness range $\text{Im}(z_0) > 0$ should hold. The symmetry exhibited by the response curves shown in Figure 5 also suggests that $\text{Re}(z_0) \approx \text{Re}(z_p)$ for the full range of thicknesses considered.

The discussion of the previous paragraph assumes the validity of the model for the case of ATR structures with metamaterials, a hypothesis that in fact has never been validated. To verify this hypothesis we have calculated numerically the parametric trajectories of $z_0(d/\lambda)$ and $z_p(d/\lambda)$. As shown in Figures 6 and 7, the obtained results are in complete agreement with these predictions and

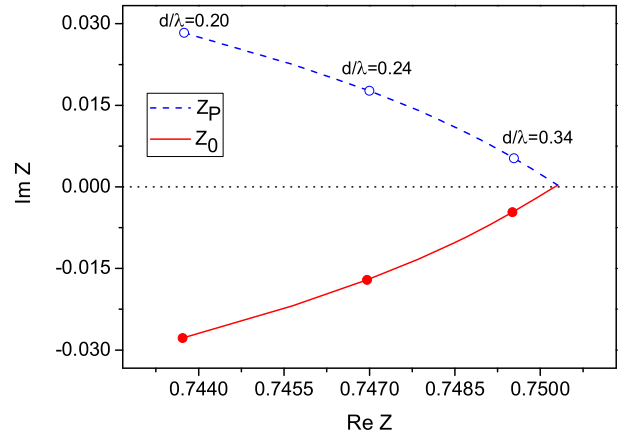


Fig. 6. (Color online) Trajectories of the zero (z_0) and the pole (z_p) in the complex plane as functions of d/λ . Constitutive parameters correspond to regime A, p -polarization, forward SPP.

confirm the validity of the model to describe phenomenologically the resonant response of SPPs in ATR structures with metamaterials. In these figures we note that the pole and zero trajectories start from the point corresponding to a single interface ($d \rightarrow \infty$) where $z_p = z_0 = 0.75030 + i0.00031$. When d/λ decreases, z_0 and z_p move away from each other, keeping their real parts approximately equal, as suggested by the symmetry of the response curves. We have also verified that

$$z_0(d/\lambda = 0.5540) = 0.75025 - i1.29559 \cdot 10^{-6},$$

$$z_0(d/\lambda = 0.5545) = 0.75025 + i7.33953 \cdot 10^{-7},$$

that is, as suggested by the change in phase behavior, the imaginary part of z_0 changes its sign at a critical value of d/λ between $d/\lambda = 0.5540$ and $d/\lambda = 0.5545$, for which the reflectivity of the system is null.

3.2 Case 2: s -polarization, backward SPPs

In our second example, the metamaterial constitutive parameters are $\varepsilon_2 = -1.5 + i0.001$ and $\mu_2 = -0.8 + i0.001$ corresponding to region B in Figure 4, where backward SPPs occur in s -polarization. In the limit $d \rightarrow \infty$ the SPP dimensionless propagation constant is $\kappa_\infty = 1.24720 - i0.00355$, with a negative imaginary part due to the SPP regressive nature. If we assume that $\kappa(d/\lambda) \approx \kappa_\infty$, equation (3) predicts a resonant coupling between the SPP and the incident wave for an angle of incidence $\theta \approx 56^\circ$.

Figure 8 shows plots of the reflectivity $|r_1(\theta)|^2$ and the phase $\phi(\theta)$ for different values of the thickness to wavelength ratio ($d/\lambda = 0.5125, 0.8145, 0.8150$ and 0.9375). The reflectivity curves for $d/\lambda = 0.8145$ and $d/\lambda = 0.8150$ are indistinguishable and present very pronounced dips, approximately equal to 10^{-7} . From the reflectivity curves (Fig. 8a) we note that both the angular position of the minima and the angular width of the dips decrease when d/λ increases. This indicates that both the real and the

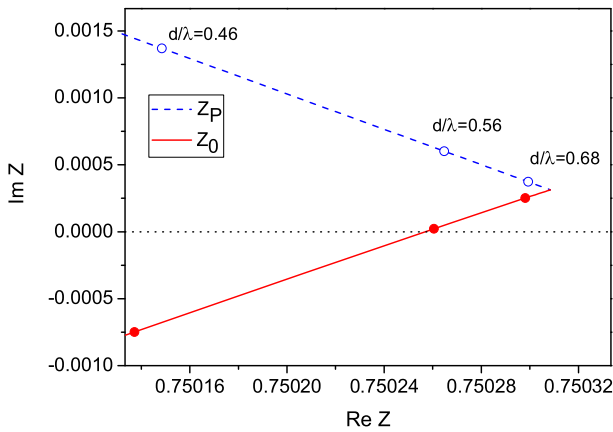


Fig. 7. (Color online) Detail of the trajectories of the zero (z_0) and the pole (z_p) in the complex plane as functions of d/λ . Constitutive parameters correspond to regime A, p -polarization, forward SPP.

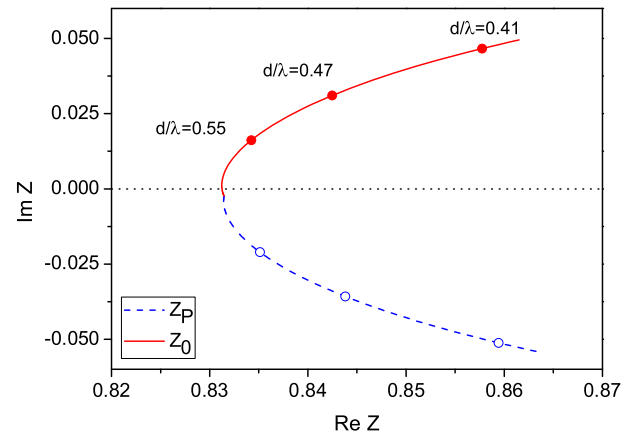


Fig. 9. (Color online) Trajectories of the zero (z_0) and the pole (z_p) in the complex plane as a function of d/λ . Constitutive parameters correspond to regime B, s -polarization, backward SPP.

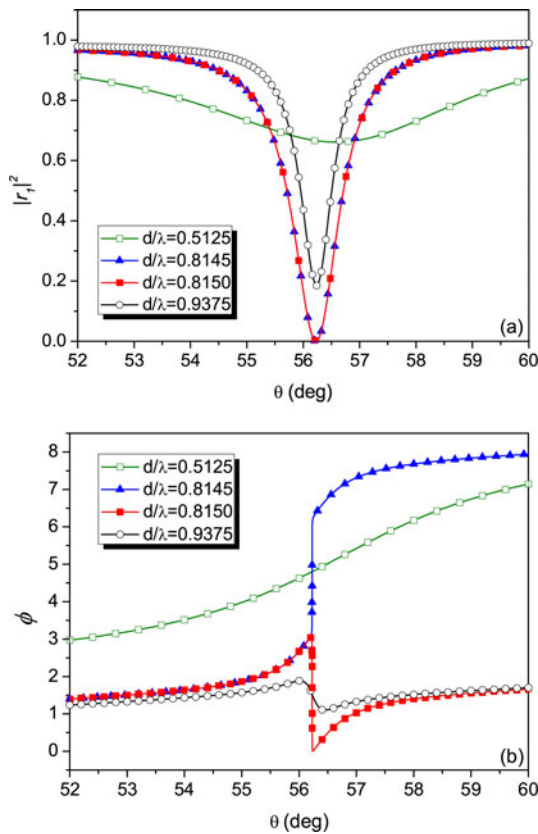


Fig. 8. (Color online) (a) Reflectivity $|r_1(\theta)|^2$ and (b) phase shift $\phi(\theta)$ as functions of the angle of incidence θ and for different values of the thickness to wavelength ratio d/λ . The relative constitutive parameters correspond to regime B.

imaginary part of the SPP constant decrease when the thickness of the metamaterial increases, in total agreement with the results in Figures 6a and 6b in [12].

The phase curves vs angle of incidence (Fig. 8b) show a very different behavior to that observed in the case discussed previously. As d/λ increases, the phase curves change from monotonously increasing, for $d/\lambda = 0.5125$

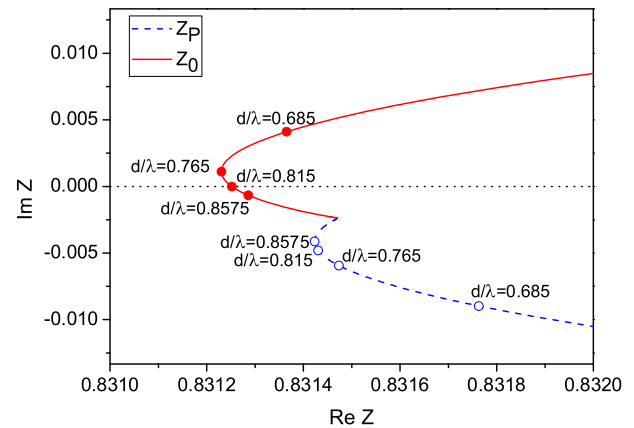


Fig. 10. (Color online) Detail of the trajectories of the zero (z_0) and the pole (z_p) in the complex plane as a function of d/λ . Constitutive parameters correspond to regime B, s -polarization, backward SPP.

and $d/\lambda = 0.8145$, to curves exhibiting a maximum and a minimum for $d/\lambda = 0.8150$ and $d/\lambda = 0.9375$. The change in the phase behavior indicates the existence of a critical value of d/λ between 0.8145 and 0.8150 for which the system reflectivity is null. In the frame of the zero-pole model, the symmetry of both the reflectivity (Fig. 8a) and the phase curves (Fig. 8b) suggests that $\text{Re}(z_0) \approx \text{Re}(z_p)$, as verified in the results shown in Figures 9 and 10 obtained from the numerical calculation of poles and zeroes. Numerically we found that

$$\begin{aligned} z_0(d/\lambda = 0.8145) &= 0.83124 + i 6.79740 \cdot 10^{-6}, \\ z_0(d/\lambda = 0.8150) &= 0.83124 - i 2.30406 \cdot 10^{-6}, \end{aligned}$$

which confirms that the critical value of d/λ for which expression (1) is identically zero occurs between the values $d/\lambda = 0.8145$ and $d/\lambda = 0.8150$.

4 Conclusions

We have presented an exhaustive study of the optical response of Kretschmann-ATR systems with negative index metamaterials in conditions close to the resonant coupling between the incident field and SPPs very different from those existing in the usual metallic ATR configurations. We have seen that all the details obtained for the optical response verify and complement the information obtained in [12] about the SPP characteristics. As a new result, our numerical simulations show that the incident field can be completely absorbed by the ATR structure when the thickness of metamaterial takes a critical value. The results of this study highlight the fact that the phase of the reflected field gives additional information not provided by the reflectivity. In particular, it has been shown that the study of the phase is useful for finding the critical conditions of total absorption. While the analysis of the optical response of the ATR system could have been done exclusively from the exact expressions of the reflection coefficient of the system, we have complemented the analysis through the extension to metamaterials of the phenomenological model previously used for ATR configurations with metals. The generalization of the model shows, in a very simple way, the key role played by SPPs in different optical responses obtained under resonance conditions.

The authors acknowledge the financial support of Consejo Nacional de Investigaciones Científicas y Técnicas, (CONICET, PIP 1800) and Universidad de Buenos Aires (project UBA 20020100100327).

References

1. *Surface Polaritons: Electromagnetic Waves at Surfaces and Interfaces*, edited by V.M. Agranovich, D.L. Mills (North-Holland, Amsterdam, 1982)
2. *Electromagnetic surface modes*, edited by A.D. Boardman (Wiley, New York, 1982)
3. W.L. Barnes, A. Dereux, T.W. Ebbesen, *Nature* **424**, 824 (2003)
4. H. Raether, *Surface Plasmons on Smooth Rough Surface and on Gratings* (Springer-Verlag, Berlin, 1988)
5. S.A. Maier, *Plasmonics: Fundamentals and Applications* (Springer-Verlag, New York, 2007)
6. R. Marqués, F. Martín, M. Sorolla, *Metamaterials with Negative Parameters: Theory, Design and Microwave Applications* (Wiley, New York, 2008)
7. L. Solymar, E. Shamonina, *Waves in metamaterials* (Oxford Univ. Press, Oxford, New York, 2009)
8. M. Cuevas, R.A. Depine, *Phys. Rev. Lett.* **103**, 097401 (2009)
9. S.A. Darmanyan, M. Nevière, A.A. Zakhidov, *Opt. Commun.* **225**, 233 (2003)
10. A. Otto, *Z. Phys.* **216**, 398 (1968)
11. E. Kretschmann, *Z. Phys.* **241**, 313 (1971)
12. M. Zeller, M. Cuevas, R.A. Depine, *J. Opt. Soc. Am. B* **28**, 2042 (2011)
13. K. Park, B.J. Lee, C. Fu, Z.M. Zhang, *J. Opt. Soc. Am. B* **22**, 1016 (2005)
14. R. Ruppini, *Phys. Lett. A* **277**, 61 (2000)
15. I.V. Shadrivov, R.W. Ziolkowski, A.A. Zharov, Y.S. Kivshar, *Opt. Express* **13**, 481 (2005)
16. A. Ishimaru, S. Jaruwatanadilok, Y. Kuga, *Prog. Electromagn. Res.* **51**, 139 (2005)
17. J.N. Gollub, D.R. Smith, D.C. Vier, T. Perram, J.J. Mock, *Phys. Rev. B* **71**, 195402 (2005)
18. K.L. Tsakmakidis, C. Hermann, A. Klaedtke, C. Jamois, O. Hess, *Phys. Rev. B* **73**, 085104 (2006)
19. R.A. Depine, V.L. Brudny, J.M. Simon, *Opt. Lett.* **12**, 143 (1987)
20. R.A. Depine, V.A. Presa, J.M. Simon, *J. Mod. Opt.* **36**, 1581 (1989)
21. M. Cuevas, R.A. Depine, *Phys. Rev. B* **78**, 125412 (2008)
22. M. Nevière, *Electromagnetic Theory of gratings*, edited by R. Petit (Springer-Verlag, Berlin, 1980), pp. 123–157
23. M.C. Hutley, D. Maystre, *Opt. Commun.* **19**, 431 (1976)
24. Y.P. Bliokh, J. Felsteiner, Y.Z. Slutsker, *Phys. Rev. Lett.* **95**, 165003 (2005)
25. W. Lukosz, H. Wahlen, *Opt. Lett.* **3**, 88 (1978)